

Endocytosis of Simian Virus 40 into the Endoplasmic Reticulum

Jürgen Kartenbeck,*[‡] Hans Stukenbrok,* and Ari Helenius*

*Department of Cell Biology, Yale School of Medicine, New Haven, Connecticut 06510; and

[‡]Institute of Cell and Tumor Biology, German Cancer Research Center, D-6900 Heidelberg, Federal Republic of Germany

Abstract. The endocytosis of SV-40 into CV-1 cells was studied using biochemical and ultrastructural techniques. The half-time of binding of [³⁵S]methionine-radiolabeled SV-40 to CV-1 cells was 25 min. Most of the incoming virus particles remained undegraded for several hours. Electron microscopy showed that some virus entered the endosomal/lysosomal pathway via coated vesicles, while the majority were endocytosed via small uncoated vesicles. After infection at high

multiplicity, one third of total cell-associated virus was observed to enter the ER, starting 1–2 h after virus application. The viruses were present in large, tubular, smooth membrane networks generated as extensions of the ER. The results describe a novel and unique membrane transport pathway that allows endocytosed viral particles to be targeted from the plasma membrane to the ER.

MANY animal viruses exploit the endocytic and secretory pathways of their host cells for entry and exit. Receptor-mediated endocytosis via coated vesicles is often required for virus penetration (14, 20, 21). Subsequently, the secretory pathway is used by many enveloped viruses for posttranslational modification and transport of virions and structural proteins to the cell surface (10). As a rule, viruses and viral components follow common established pathways of constitutive cellular membrane traffic.

Morphological studies of SV-40 and polyoma virus entry have suggested, however, that all viruses may not be as disciplined in their interactions with cellular organelles. These nonenveloped viruses, which belong to the papovavirus family, have been seen to enter the cells via small tight-fitting, uncoated membrane vesicles ("monopinocytotic" vesicles) derived from the plasma membrane (13, 15, 19, 23, 24). Incoming virus particles have also been reported in a variety of cellular compartments, including the nucleoplasm, the lysosomes, the ER, and mitochondria (15, 19, 23, 24). SV-40 particles have also been found in the cytoplasm, where they sometimes appear between ER cisternae (24).

The apparent presence of viruses within a compartment associated with the ER (24) is particularly interesting because it suggests a novel endocytotic pathway targeted from the plasma membrane to the ER. Endocytic markers are generally not observed in the ER; they enter the endosomes and lysosomes, and some markers enter the *trans* compartment within the Golgi complex. Alternatively, as recently suggested by Clayson et al. (7), the ER-associated virus could represent newly assembled particles in transit from the nucleus (where assembly of SV-40 occurs) to the extracellular space. In this paper we have reinvestigated the uptake of SV-40 into CV-1 cells and established (a) that incoming particles are, indeed, targeted to the ER; (b) that they there induce the

formation of specialized tubular membrane structures; and (c) that initial uptake occurs mainly by adsorptive endocytosis independent of coated vesicles.

Materials and Methods

Cells and Viruses

African green monkey kidney cells (CV-1 cells) were grown in DME with 10% FCS. Cells were subcultured and split to a ratio of 1:10 and used between passages 3 and 25. They were passaged twice weekly and experiments were done on the second or third day after plating.

For stock virus production, subconfluent cells were infected with a multiplicity of 0.01 plaque-forming units (PFU).¹ For radioactive virus 10 PFU was used. Cells were grown in cell culture flasks (75 cm²; Falcon Labware, Oxnard, California). After 10–11 and 3–4 d, respectively, infected cells and supernatants were collected and frozen in 10 mM Tris-HCl, pH 7.2, and stored at –70°C. To grow SV-40 incorporating isotopically labeled DNA, the medium was replaced with fresh medium containing 20 μCi of [³H]thymidine/ml (specific activity 70–85 Ci/mmol; Radiochemical Centre, Amersham, England) 15–18 h after infection. For production of virus incorporating isotopically labeled proteins, the medium was removed 2 h after infection and replaced with medium containing 25% less of the normal methionine concentration. 25–30 h later, 50 μCi of [³⁵S]methionine (specific activity 1,000 Ci/mmol; Radiochemical Centre) was added to the medium. Virus pools used in this study contained an average of 2.5 × 10⁸ PFU/ml. The PFU were determined by plaque assay (11).

Virus Purification

Infected cells and supernatants were frozen and thawed three times and further disrupted by sonication (two bursts for 3–4 s each burst). After centrifugation at 10,000 g for 40 min, the pellet was resuspended in 10 mM Tris, pH 7.4, sonicated as above, and centrifuged at 10,000 g for 30 min. Both supernatants were combined and centrifuged at 140,000 g for 3.5 h. The pellet was resuspended in DME using a small homogenizer (Potter; Chemie

1. Abbreviations used in this paper: HRP, horseradish peroxidase; PFU, plaque-forming unit.

und Werkstoff Technik, Cti, Jolstein/Taunus, FRG) and centrifuged on a CsCl-gradient (1.34 g/cm³) at 105,000 g for 24 h. The banded virus (density ~1.38 g/cm³) was collected, dialyzed against 10 mM Tris-HCl, pH 7.4, frozen in liquid nitrogen, and stored at -70°C. The [³H]thymidine- and [³⁵S]methionine-labeled virus contained ~5 × 10³ and 9 × 10⁴, respectively, counts per 10 μl.

Association of [³⁵S]Methionine-labeled SV-40 Particles to CV-1 Cells

Confluent cells on 6-cm Petri dishes were washed twice with R medium (RPMI 1640 containing 10 mM Hepes, 0.1% BSA, pH 6.8). The medium was removed, and 1 ml of [³⁵S]methionine-labeled SV-40 in R medium was added to each dish. The cells were incubated for various periods of time at 37°C; during this time the dishes were rocked slowly. For later time points than 120 min, the R medium was removed, the cells were washed twice with R medium, and 5 ml of fresh DME was added. To determine total cell-associated radioactivity, the medium was removed, and the cells were washed twice, scraped into 1 ml PBS containing 1 mM PMFS, precipitated with TCA (for 1 h at 0°C at a final concentration of 10%), and centrifuged (for 15 min at 5,000 rpm at 4°C). The dishes were subsequently washed twice with 1 ml 10% TCA. The collected precipitates were assayed for radioactivity. Treatment of cell surface-associated virus was performed using proteinase K as described (14). Aliquots of the combined medium and washes were precipitated with TCA for determination of degraded viral proteins (as above).

Gel Electrophoresis

Cells were scraped off the dish with PBS (containing 2% FCS, 1 mM PMFS, Aprotinin), centrifuged, and dissolved in Laemmli sample buffer (17). Gels (10%) were prepared according to Laemmli (17). Fluorography was performed essentially by the method of Chamberlain (5) using 1 M sodium salicylate, pH 7, in 30% methanol.

Electron Microscopy

For morphological studies, confluent cells were either grown on coverslips or in 12-well Linbro plates (Flow Laboratories, Hamden, CT). Before infection with SV-40, the cells were washed twice with R medium. Infection with unlabeled and [³H]thymidine-labeled virus was performed at a multiplicity of 0.5–5 × 10³ PFU/cell at 37°C. R medium was used for time points up to 60 min. For later time points, R medium was replaced by DME. Endocytosis of soluble type VI horseradish peroxidase (HRP; Sigma Chemical Co., St. Louis, MO) was performed as described (31). For experiments with cycloheximide (2–20 μg/ml; Sigma Chemical Co.), the inhibitor was either applied with the virus or 2 h after infection and left in the culture medium until the end of the experiment. At different time points after infection, cells were fixed for electron microscopy in 2.5% glutaraldehyde (0.05 M sodium cacodylate, pH 7.2, 50 mM KCl, 1.25 mM MgCl₂, 1.25 mM CaCl₂) for 20 min at room temperature followed by 1 h in 2% OsO₄. Dehydration, embedding, thin sectioning, staining, and autoradiography were performed as described (16, 28). Electron micrographs were taken with a JEOL USA 100 electron microscope (Peabody, MA) and a Philips Electronic Instruments, Inc., 400 electron microscope (Mahwah, NJ). For quantitative analysis, either micrographs were taken at a primary magnification of 10,000× or the cells were observed under the electron microscope at a magnification of 25,000×. Statistical evaluation was done on sections of 250 complete cells of duplicate experiments.

Electron Microscopic Immunolocalization

For immunolocalization, cells were fixed for 20 min in 3% freshly prepared formaldehyde in PBS, pH 7.2, followed by a brief treatment with 0.5% saponin in PBS for 3 min. A murine monoclonal antibody (4) specifically recognizing a component of the ER (binding protein BiP, also called GRP 78; see reference 4; generously provided by Dr. D. Bole, Yale University Medical School, New Haven, CT) was applied for 3 h. The reactive sites were visualized by application of a secondary goat anti-mouse antibody coupled to HRP (Biomed, Hamburg, FRG) for 40 min. Reaction with diaminobenzidine was performed as described (12, 16).

Results

The kinetics of SV-40 binding to CV-1 cells was determined

using isolated [³⁵S]methionine-labeled virus. As shown in Fig. 1 *a* the half-time of association at 37°C was ~25 min, which is comparable with other animal viruses under similar conditions (22). The association was virtually irreversible: the viruses could not be removed by repeated washing and only 10% could be removed at any time by proteinase K digestion. Degradation of cell-associated viral proteins was remarkably slow compared with viruses that enter the endosomal/lysosomal pathway (22). Only 5% was degraded during the first 2 h as judged by the small amount of TCA-soluble radioactivity generated (Fig. 1 *a*). After 22 h, 65% of the structural proteins VP1 and VP3 remained intact (Fig. 1, *b* and *c*). This suggested that the majority of SV-40 particles either remained extracellular for extended periods of time or that the virus entered the cell but escaped degradation.

To further trace the fate of the virus particle, electron microscopy was used. SV-40 was added to CV-1 cells at high multiplicity, and the cultures were fixed for electron microscopy after incubation at different times at 37°C. After short incubations (5–10 min), the virus particles were seen attached to the cell surface. As previously described (13, 15, 19, 24), many viruses were in small invaginations and at the plasma membrane, and some were in tight-fitting monopinoscytotic vesicles (Fig. 2, *a–c*; reference 13). These vesicles had a diameter of 60 nm, and there was no visible coat material on their cytoplasmic surface. Occasional virus particles could also be seen in typical coated pits and coated vesicles (Fig. 2 *d*). After 15–30 min of incubation, viruses were increasingly observed within tubular membrane-bounded structures (Fig. 2 *e*) that often contained multiple viral particles. Some viruses were also present in endosomes (Fig. 2, *g* and *h*). We observed no difference in the uptake of complete viruses and empty capsids present in some of our virus preparations. The latter can be easily distinguished by the lack of an electron-dense central core (see Fig. 2, *e* and *j*).

After 1–2 h, virus particles and empty capsids began to appear in the lumen of the ER. Initially they were mostly present as single isolated particles, but over the next few hours irregular, ER-associated, tubular membrane networks appeared containing a large number of particles (Fig. 2, *f*, *i*, and *j*). The viruses typically occupied positions in the vertices of the complex tubular structure. In many instances, the virions defined the point of convergence of three to six separate tubular membrane elements radiating in different directions. The membranes of these structures were devoid of ribosomes (24), but they were in direct continuity with the RER. The ER aggregates were found with a frequency of 0.7 aggregates per cell section. This number remained unchanged after 4–22 h of incubation, but the number of virus particles and the size of the aggregates increased with time. Some reached a size of 1–2 μm in diameter as shown in Fig. 3 *b*. Several large virus-containing clusters could be seen in a single cell (Fig. 3 *a*).

In rare cases, virus particles were also seen in the space between the outer and inner nuclear membranes (Fig. 2 *k*; see also 24). In contrast to previous reports (24), we did not detect delivery of viruses into mitochondria, the nucleoplasm, or the cytoplasm; viruses were also not apparent in the Golgi stacks. While common in endosomes, virus particles were rarely seen in typical secondary lysosomes.

To confirm that the virus-containing tubular membrane networks were part of the ER, immunocytochemistry was

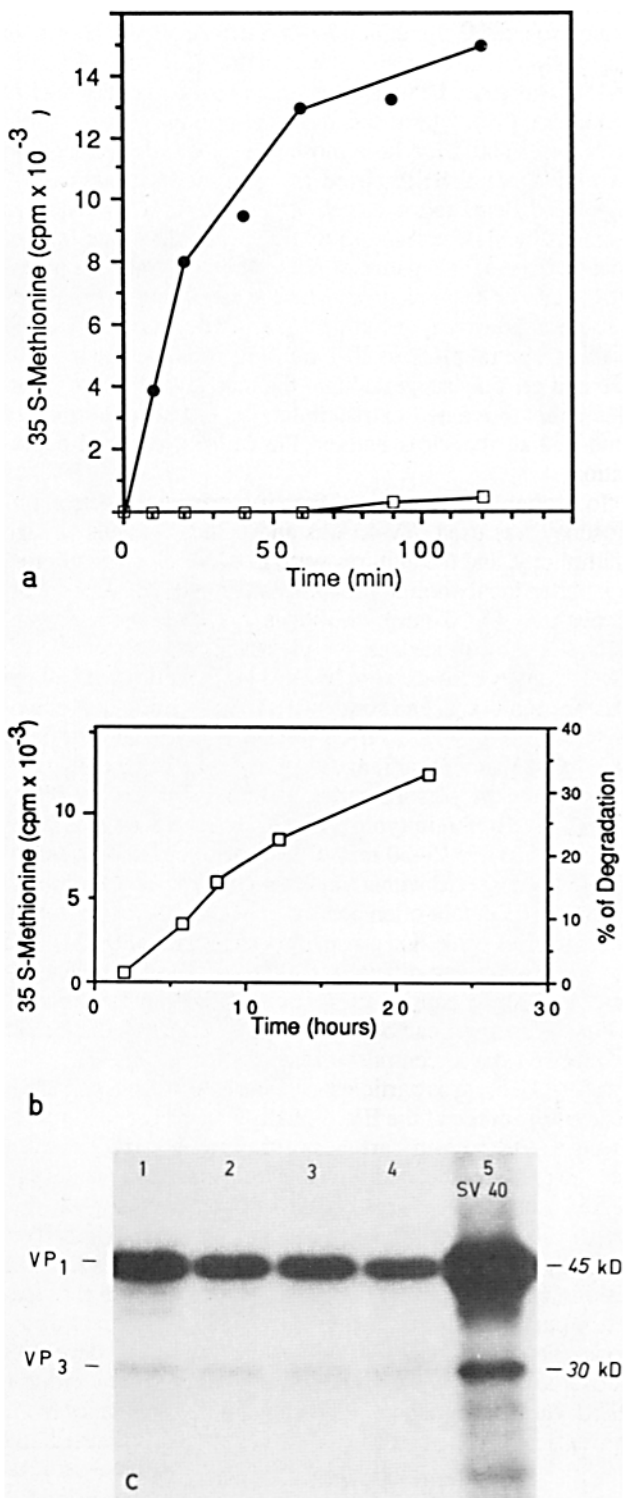


Figure 1. SV-40 interaction with CV-1 cells at 37°C. (a) Total cell association of ^{35}S -SV-40 is indicated by solid circles. Degraded viral proteins, indicated by open squares, were detected by determination of acid-soluble radioactivity in the binding medium. Cells (7×10^6 on 6-cm dishes) were incubated with 24,000 cpm ^{35}S -SV-40 (6.4×10^8 PFU). (b) Kinetics of ^{35}S -SV-40 degradation between 2 and 22 h after infection. After binding of the virus in R medium for 2 h, unbound virus was washed away and R medium was replaced with cold culture medium. Degraded viral proteins (acid-soluble radioactivity in the medium) were determined at the indicated time points. Cells (7×10^6 on 6-cm dishes) were incubated with 60,000 cpm ^{35}S -SV-40 (9×10^8 PFU). (c) ^{35}S -SV-40 was ap-

plied to CV-1 cells for 2 h at 37°C. Unbound virus was washed away, and cells were collected at various time points after infection and resolved on a 10% Laemmli gel. (Lanes 1-4) 2, 6, 23, and 46 h after infection, respectively. Note the presence of the intact viral core proteins VP1 and VP3 even at late time points of infection. (Lane 5) Virus fraction used for infection (SV-40).

performed using antibodies to a binding protein (BiP, also called GRP 78). This heat shock-related soluble protein is located within the ER (4). The immunoperoxidase technique showed that the virus-containing ER structures contained BiP (Fig. 4). Although the resolution was not optimal (a frequent problem with this technique in CV-1 cells), it was clear that BiP was ER specific; no staining of Golgi cisternae, mitochondria, and endocytic organelles was detected.

To obtain a quantitative estimate of the virus distribution in the cell, morphological quantitation was performed on random sections. The number of viruses was determined in five compartments: the plasmamembrane; the monopinocytotic vesicles; the tubular structures; the endosomes, lysosomes, multivesicular bodies, and larger vacuoles; and the ER. The results shown in Fig. 5 revealed that at intermediate times many viruses were seen in monopinocytotic vesicles, tubular structures, and endosomes. After 4 h, intracellular viruses were mainly in the tubular structures, and, at 19 h (and beyond), the majority of the virus particles (55%) had moved from the surface to the ER-associated structures. Thus, transport to the ER occurred rather slowly.

Three methods were used to confirm that the ER-associated viruses were endocytically derived and not newly synthesized progeny viruses. First, ^3H -labeled viruses were allowed to enter and the cells were analyzed by electron microscopic autoradiography. The label was observed over all the virus-containing ER aggregates (Fig. 6) and over some endosomes (not shown). A few grains were also seen over the nucleus and over cytoplasmic areas devoid of identifiable virions. As shown in Fig. 6 b, the progeny viruses in the nucleus were not labeled. Mitochondria and the Golgi complexes were similarly devoid of radioactive label (e.g., Fig. 6 a). Second, viruses were allowed to enter cells in the presence of cycloheximide. Despite the block in protein synthesis, virus particles appeared in the ER lumen and in ER aggregates. Third, cells were infected at low (less than one) multiplicity of infection and allowed to synthesize viruses for 48-60 h. Under these conditions, no ER aggregates were observed. We conclude from these experiments that the viruses in the ER constitute endocytosed particles and that formation of the tubular ER structures is independent of protein synthesis. This conclusion is in agreement with the observation that ER particles appear well before the onset of progeny virus production. In addition, it is apparent that newly synthesized viruses abundantly present in the nucleus cannot enter the ER cisternae.

As already mentioned, markers of fluid or adsorptive endocytosis do not normally reach the ER (31, 32). To test whether a fluid phase marker could enter together with the incoming virus particles, virus uptake was allowed to occur in the presence of 1 mg/ml HRP. We found that, while virus entered normally, no HRP staining could be detected in the ER compartment. Endosomes and lysosomes were, however, as strongly stained as in control cells (Fig. 7). These

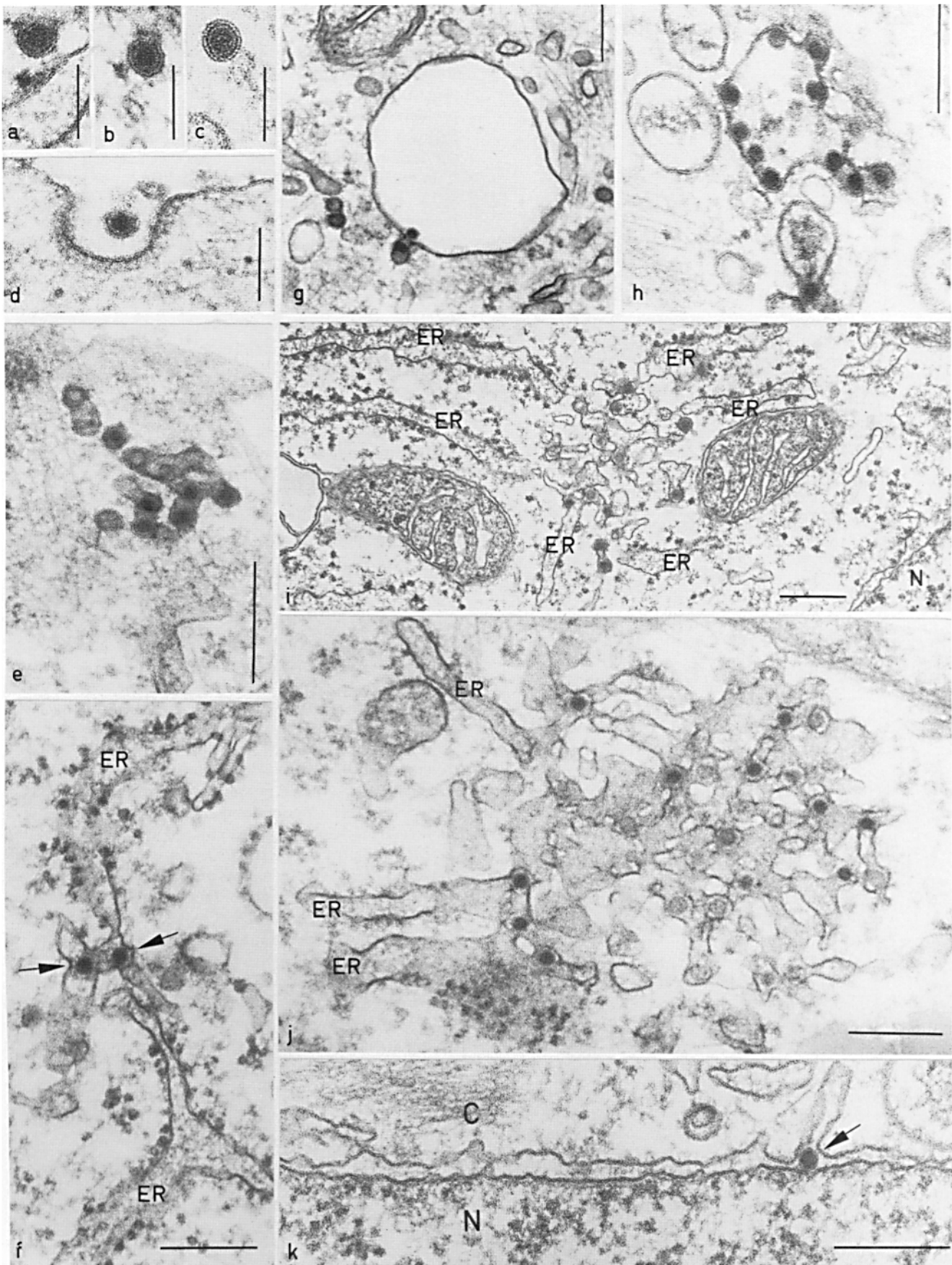


Figure 2. Early events (10–20 min after infection) in CV-1 cells infected with SV-40 demonstrate the “budding-like” internalization and the formation of tightly enveloped virus particles (a–c), which seem to accumulate, fuse, and eventually to form short, branching tubular membrane structures (e). Occasionally, virus particles could be seen in coated pits (d). Virus particles (f, arrows) are found in the cisternae of the ER (ER) or in anastomosing, irregularly shaped membranous structures, regularly surrounded by projecting ER cisternae (i and j), some of which are in a membrane continuity with the forming aggregates (i and j). A single virus particle (arrow) inside the cisterna of the nuclear membrane is shown in j. C, cytoplasm; N, nucleoplasm. Time after infection: (a–e) 10–20 min; (f) 4 h; (g) 19 h; (h) 6 h; (i) 16 h; (j) 19 h. Bars: (a–d) 0.1 μm ; (e–j) 0.2 μm .

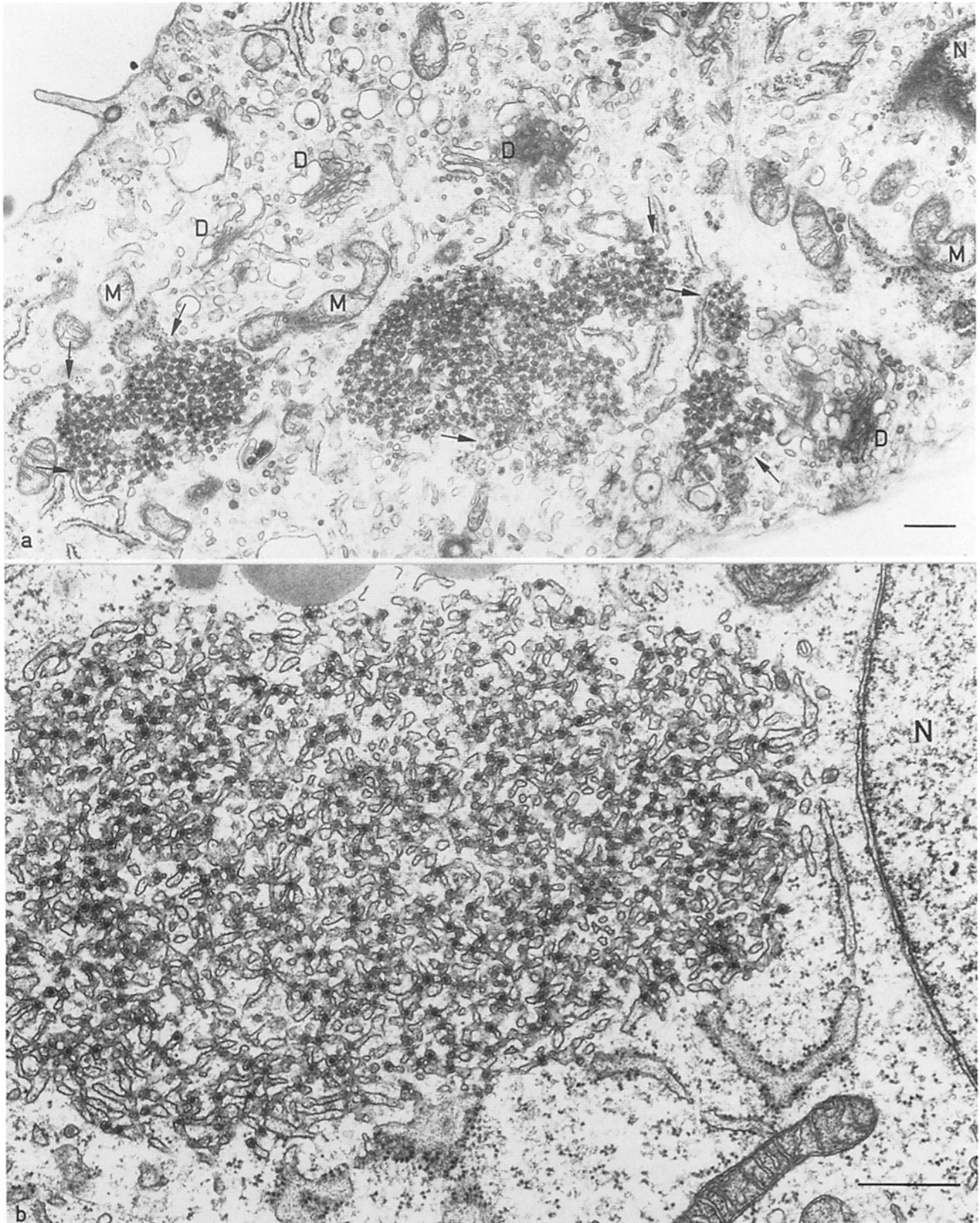


Figure 3. (a) Survey micrograph of a CV-1 cell with several virus-containing aggregates 16 h after infection, each of them in the vicinity of a dictyosome (D). Arrows point to membrane continuities between the RER and the aggregates. At higher magnification (b), an extended network of tubular, anastomosing membranes containing abundant virus particles is shown. Note the absence of virus particles in the cell nucleus (N) and on the cell surface. Bars, 0.5 μm .

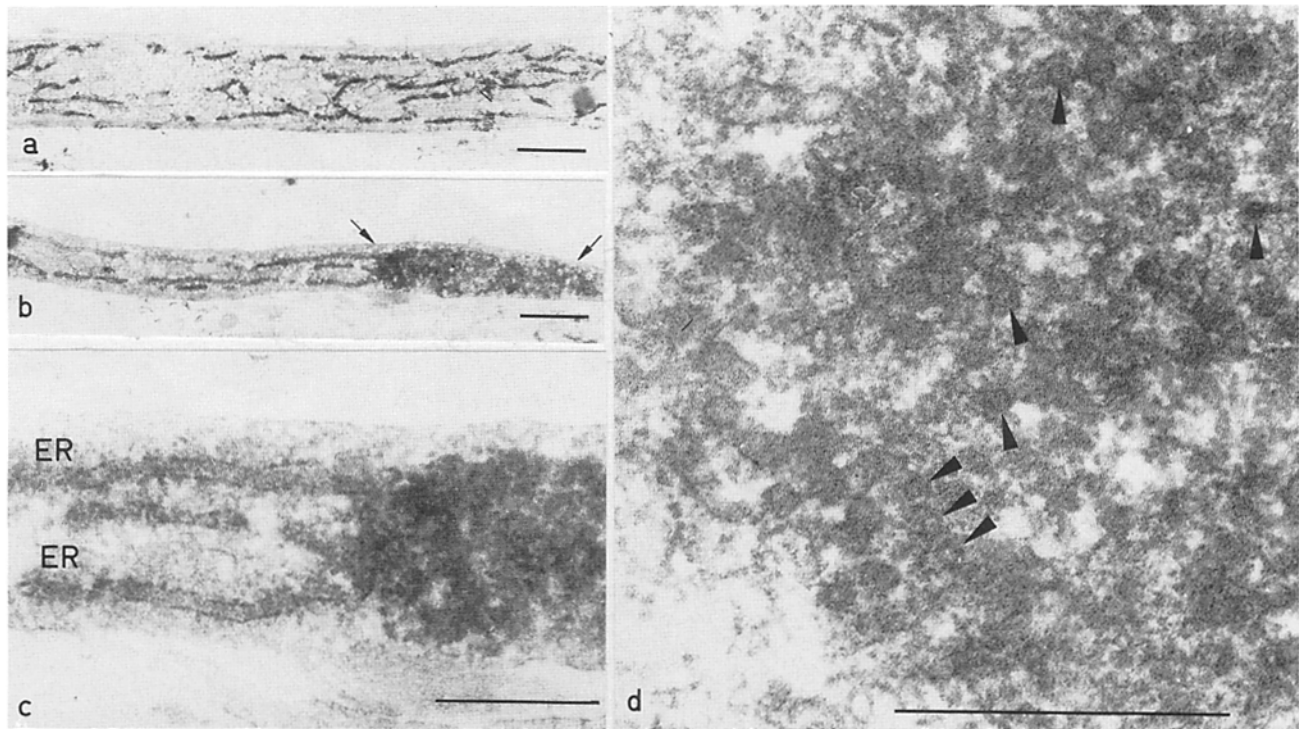


Figure 4. Immunoperoxidase cytochemistry using BiP antibody (4) recognizing components of the ER (ER). Reaction products are seen in all cisternae of the ER (a-c) including the virus-containing aggregates (b, arrows). At higher magnification, individual virus particles can be detected, some of them are denoted by arrowheads (e). Bars, 0.5 μ m.

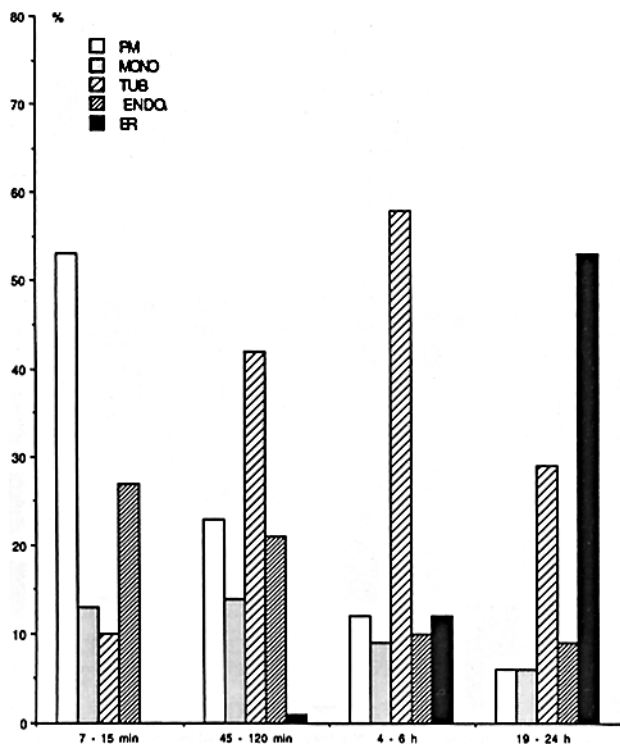


Figure 5. Quantitation of internalized SV-40 particles on random sections of CV-1 cells by electron microscopy. The columns represent the relative amount of internalized virus as found in five classified membrane compartments at different time points after infection. Results represent the average of duplicate experiments. Open columns indicate viral particles tightly attached to the plasma membrane (PM). Dotted columns indicate monopinocytotic ves-

icles (MONO). Tubular structures (TUB) are indicated by the coarsely hatched columns, and the endosomes, multivesicular bodies, lysosomes, and larger vacuoles (ENDO) are indicated by the finely hatched columns. Black columns represent virus present in ER cisternae and tubular membrane networks forming membrane continuities with the ER (ER).

Discussion

It is clear from the results in this paper and from several previous studies (15, 23, 24) that SV-40 particles and other papovaviruses enter the host cell by endocytosis. This occurs in part via the constitutive receptor-mediated pathway involving coated vesicles, endosomes, and lysosomes or a pathway commonly used by other viruses for cell entry and infection (22). A large fraction of the SV-40 particles, however, follow a less conventional endocytic pathway that begins with the inclusion into tight-fitting plasma membrane-derived vesicles (15, 23, 24). Morphological and biochemical studies of these monopinocytotic vesicles (13) have suggested that they may be formed as a consequence of tight binding of the virus to multiple, yet unidentified, plasma membrane receptors. Our results suggest that the fit between the virus and the vesicle membrane is apparently so tight that there is little space for fluid markers. This is in marked contrast to coated vesicle-dependent endocytosis of Semliki Forest virus, which is accompanied by detectable amounts of fluid uptake (21).

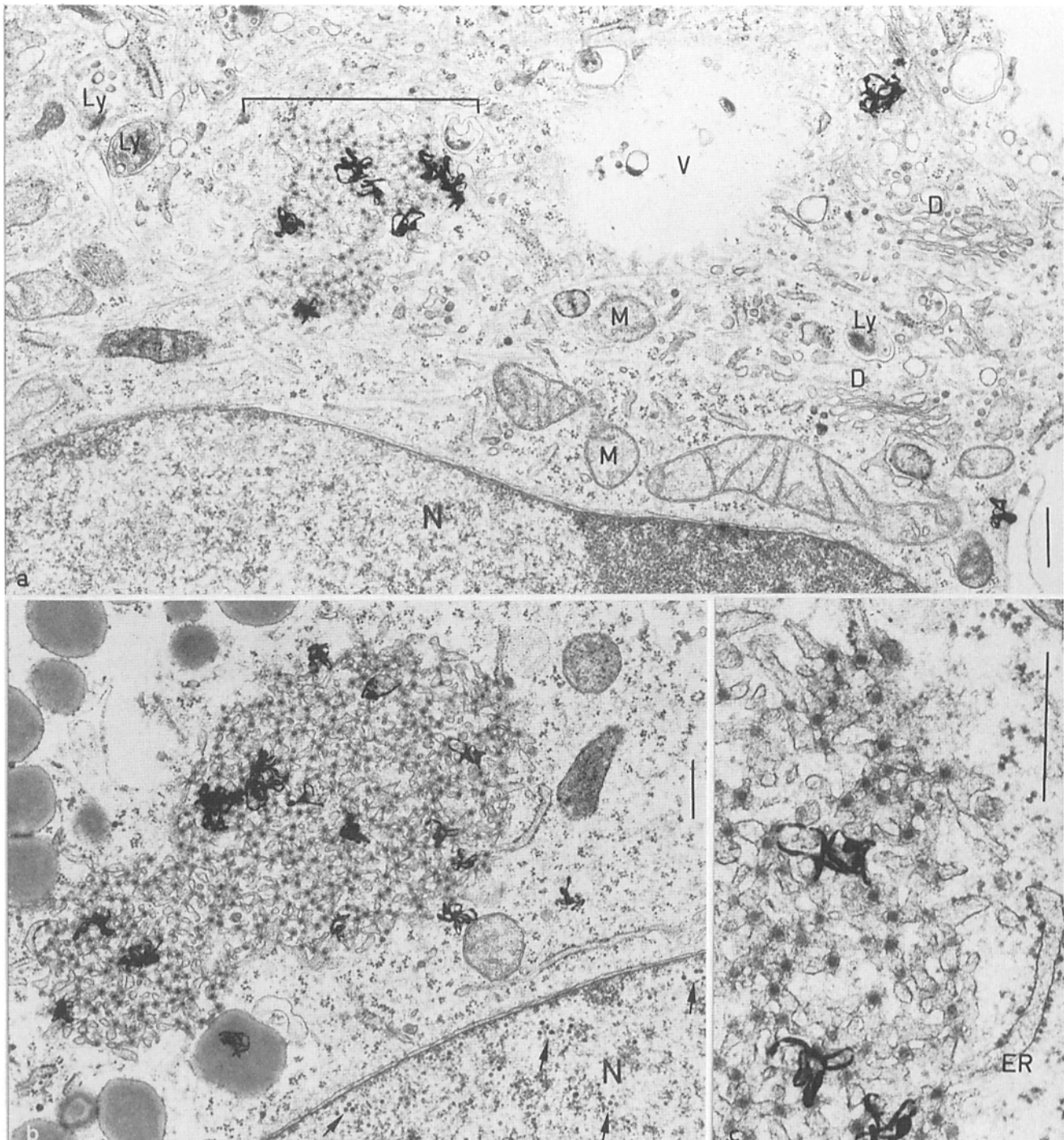


Figure 6. Electron microscopic autoradiography of CV-1 cells infected for 19 h with [^3H]thymidine-labeled SV-40. Silver grains are seen over all virus-containing aggregates (*a*, *bracket*, and *b* and *c*) and occasionally free over the cytoplasm (*a*). No grains were seen over dictyosomes (*D*), mitochondria (*M*), lysosomes (*Ly*), vacuoles (*V*), or progeny virus (*b*, *arrows*) in the cell nucleus (*N*). Bars, 0.5 μm . An ER cisternae demonstrating a membrane continuity with an aggregate is shown at higher magnification in *c*.

The most striking aspect of the SV-40 uptake is the targeting to the ER since the ER is not generally considered an acceptor organelle for endocytotic membrane traffic. A variety of tracers such as HRP, cationized ferritin, and gold-labeled ligands are routinely seen to enter endosomes, lysosomes, multivesicular bodies, and other elements of the vacuolar apparatus (31, 32). Internalized compounds, though less fre-

quently, also enter Golgi elements (2, 34, 35). Such commonly used markers as well as receptor-bound ligands of endocytosis are, however, conspicuously absent from the ER, nuclear membrane, and mitochondria. The observation that SV-40 is delivered to the ER is, therefore, unique. Whether the transport reflects an ongoing process that the virus exploits or an individual pathway specific for the virus

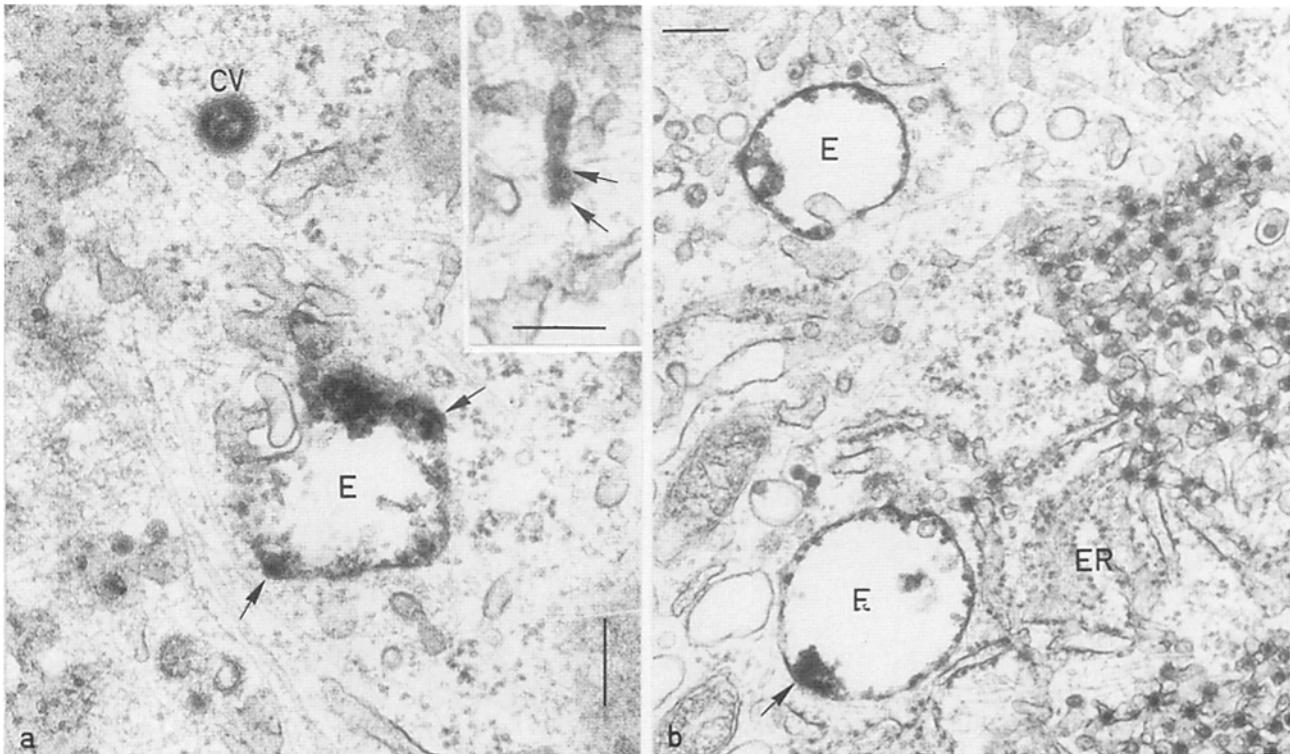


Figure 7. Electron micrographs of CV-1 cells infected with SV-40 and exposed to HRP. Cells infected for 90 min with SV-40 followed by a pulse of HRP for 20 min (a) show reaction products in coated vesicles (CV), endosomes (E), and some tubular structures (insert). In b, cells 6 h after infection with SV-40 were exposed for an additional 16 h to HRP. Reaction products are found in various membrane compartments of the endocytotic pathway, as shown here in endosomes (E) but not in cisternae of the ER or in the extended tubular networks that form membrane continuities with the ER. Arrows point to internalized virus particles that are partly obscured by the electron-dense reaction product. Bars, 0.2 μm .

is not known. However, the pinocytotic vesicles involved must contain components that allow their targeting to the ER. Additional studies may allow the identification of such factors. Also, viruses may provide a mechanism for transporting membrane-impermeable reagents to the ER: such compounds could include pH probes, inhibitors, peptides, and proteins.

The notion that the ER can serve as an acceptor compartment for membrane transport, and not only as a donor, has been recently discussed in the context of lipid recycling and the replacement of membrane lost from the ER during secretion (26). The recent papers of Lippincott-Schwartz et al. (18) and Doms et al. (9) suggest that a membrane recycling can indeed occur between *cis*- and *medial*-Golgi cisternae and the ER. Whether transport to the ER can occur from more distal organelles such as the plasma membrane is not clear. It is known that certain lipids such as cholesterol and desmosterol, when applied extracellularly, do reach the ER where they become metabolically modified (30).

The ER-associated virus particles were present in elaborated interconnected, tubular smooth membrane structures. Such specializations of the ER, though structurally somewhat different, have previously been described in cells chronically starved of cholesterol as well as in cells treated with inhibitors such as 3-hydroxy-3-methylglutarylcoenzyme A reductase (6, 25, 29). They have also been observed in type II cells of the taste buds (33) and in some cell types infected with other viruses (27). Thus, the ER is an organelle that can accommodate large amounts of newly synthesized membrane

proteins such as the coenzyme A reductase but also massive amounts of endocytosed virions. It may be significant that the virus-containing structures contain the heat shock protein BiP, which has been implicated as a cofactor during protein oligomerization and the retention of misfolded proteins within the ER lumen (4). In agreement with immunolocalization data by Bole, D., and J. D. Jamieson (Yale University Medical School, New Haven, CT; personal communication), BiP was exclusively observed within the ER system of CV-1 cells, thereby confirming that the virions were within the ER.

Our results indicate that the ER contains incoming endocytosed particles and not progeny virus derived from the cell's nucleus. It is therefore unlikely that the ER structures serve in the transit of newly synthesized SV-40 from the nucleus to the plasma membrane, as recently suggested by Clayson et al. (7) for polarized epithelial cells. However, it is also unclear whether the transport of viruses to the ER is in any way connected with productive infection of the cell.

To infect a host cell, SV-40 has to deliver its genome to the nucleus, which is the site of papovavirus replication, transcription, and virion assembly. Only a small fraction of papovavirus particles are capable of initiating infection (1, 3, 8), and preliminary results indicate that only 5–10% of viral DNA is delivered to the nucleus. Additional studies must address the possible mechanisms by which the viral genome could be translocated from the ER to nuclear compartment.

We thank Dr. David Bole for the gift of monoclonal anti-BiP antibody, Dr. Michael Walsh and Mark Paulik for critical reading of the manuscript, and E. Gundel for careful typing of the manuscript.

These studies were supported by grants from the Deutsche Forschungsgemeinschaft and from the National Institutes of Health (AI18599).

Received for publication 7 February 1989 and in revised form 12 July 1989.

References

1. Acheson, N. H. 1980. Lytic cycle of SV40 and polyoma virus. In *DNA Tumor Viruses*. J. Tooze, editor. Cold Spring Harbor Laboratory, Cold Spring Harbor, NY. 125-204.
2. Balin, B. J., and R. D. Broadwell. 1987. Lectin-labeled membrane is transferred to the Golgi complex in mouse pituitary cells in vivo. *J. Histochem. Cytochem.* 35:489-498.
3. Black, P. H., E. M. Crawford, and L. V. Crawford. 1964. The purification of simian virus 40. *Virology*. 24:381-387.
4. Bole, D. G., L. M. Hendershot, and J. F. Kearney. 1986. Posttranslational association of immunoglobulin heavy chain binding protein with nascent heavy chains in nonsecreting and secreting hybridomas. *J. Cell Biol.* 102:1558-1566.
5. Chamberlain, J. P. 1979. Fluorographic detection of radioactivity in polyacrylamide gels with the water-soluble fluor, sodium salicylate. *Anal. Biochem.* 98:132-135.
6. Chin, D. J., K. L. Lusky, R. G. W. Anderson, J. R. Faust, J. L. Goldstein, and M. S. Brown. 1982. Appearance of crystalloid endoplasmic reticulum in compactin-resistant Chinese hamster cells with a 500-fold increase in 3-hydroxy-3-methylglutaryl-coenzyme A reductase. *Proc. Natl. Acad. Sci. USA*. 79:1185-1189.
7. Clayson, E. T., L. V. Jones Brando, and R. W. Compans. 1989. Release of simian virus 40 virions from epithelial cells is polarized and occurs without cell lysis. *J. Virol.* 63:2278-2288.
8. Crawford, L. V., E. M. Crawford, and D. H. Watson. 1962. The physical characteristics of polyoma virus. I. Two types of particle. *Virology*. 18:170.
9. Doms, R. W., G. Russ, and J. W. Yewdell. 1989. Brefeldin A redistributes resident and itinerant Golgi proteins to the ER. *J. Cell Biol.* 109:61-72.
10. Dubois-Dalcq, M., K. V. Holmes, and B. Rentier. 1984. Assembly of enveloped RNA viruses. Springer-Verlag, Wien, New York. 217 pp.
11. Fendrick, J. L., and L. M. Hallick. 1983. Optimal conditions from titration of SV40 by the plaque assay method. *J. Virol. Methods*. 7:93-102.
12. Graham, R. C., and M. J. J. Karnovsky. 1966. The early stages of absorption of injected horseradish peroxidase in the proximal tubules of mouse kidney: ultrastructural cytochemistry by a new technique. *J. Histochem. Cytochem.* 14:291-302.
13. Griffith, M. J., and R. A. Consigli. 1984. Isolation and characterization of monopinocytotic vesicles containing polyomavirus from the cytoplasm of infected mouse kidney cells. *J. Virol.* 50:77-85.
14. Helenius, A., J. Kartenbeck, K. Simons, and E. Fries. 1980. On the entry of Semliki Forest virus into BHK-21 cells. *J. Cell Biol.* 84:404-420.
15. Hummeler, K., N. Tomassini, and F. Sokol. 1970. Morphological aspects of the uptake of simian virus 40 by permissive cells. *J. Virol.* 6:87-93.
16. Kartenbeck, J., E. Schmid, H. Müller, and W. W. Franke. 1981. Identification and localization of clathrin and coated vesicles. *Exp. Cell Res.* 133:191-211.
17. Laemmli, U. 1970. Cleavage of structural proteins during the assembly of the head of bacteriophage T4. *Nature (Lond.)*. 227:680-685.
18. Lippincott-Schwartz, J., L. C. Yuan, J. S. Bonifacino, and R. D. Klausner. 1989. Rapid redistribution of Golgi proteins into the ER cells treated with brefeldin A: evidence for membrane cycling from Golgi to ER. *Cell*. 56:801-813.
19. Mackay, R. L., and R. A. Consigli. 1976. Early events in polyoma virus infection: attachment, penetration, and nuclear entry. *J. Virol.* 19:620-636.
20. Marsh, M. 1984. The entry of enveloped viruses into cells by endocytosis. *Biochem. J.* 218:1-10.
21. Marsh, M., and A. Helenius. 1980. Adsorptive endocytosis of semliki forest virus. *J. Mol. Biol.* 142:439-454.
22. Marsh, M., and A. Helenius. 1989. Virus entry into animal cells. *Adv. Virus Res.* 36:107-151.
23. Mattern, C. F. T., K. K. Takemoto, and W. A. Daniel. 1966. Replication of polyoma virus in mouse embryo cells: electron microscopic observations. *Virology*. 30:242-256.
24. Maul, G. G., G. Rovera, A. Vorbrodt, and J. Abramczuk. 1978. Membrane fusion as a mechanism of simian virus 40 entry into different cellular compartments. *J. Virol.* 28:936-944.
25. Orci, L., M. S. Brown, J. L. Goldstein, L. M. Garcia-Segura, and R. G. W. Anderson. 1984. Increase in membrane cholesterol: a possible trigger for degradation of HMGCoA reductase and crystalloid endoplasmic reticulum in VT-1 cells. *Cell*. 36:835-845.
26. Pfeffer, S. R., and J. E. Rothman. 1987. Biosynthetic protein transport and sorting by the endoplasmic reticulum and Golgi. *Annu. Rev. Biochem.* 56:829-852.
27. Quan, C. M., and F. W. Doane. 1983. Ultrastructural evidence for the cellular uptake of rotavirus by endocytosis. *Intervirology*. 20:223-231.
28. Salpeter, M. M., and L. Bachmann. 1970. Autoradiography. In *Principles and Techniques for Electronmicroscopy*. M. A. Hayat, editor. Van Nostrand Reinhold Co., New York. 221-278.
29. Singer, I. I., D. W. Kawka, D. M. Kazakis, A. W. Alberts, J. C. Chen, J. W. Huff, and G. C. Ness. 1984. Hydroxymethylglutaryl-coenzyme A reductase-containing hepatocytes are distributed periportal in normal and mevinolin-treated rat livers. *Proc. Natl. Acad. Sci. USA*. 81:5556-5560.
30. Slotte, J. P., and E. L. Bierman. 1987. Movement of plasma membrane sterols to the endoplasmic reticulum in cultured cells. *Biochem. J.* 248:237-242.
31. Steinmann, R. M., J. M. Silver, and Z. A. Cohn. 1974. Pinocytosis in fibroblasts: quantitative studies in vitro. *J. Cell Biol.* 63:949-969.
32. Steinmann, R. M., R. S. Mellmann, W. A. Müller, and Z. A. Cohn. 1983. Endocytosis and the recycling of the plasma membrane. *J. Cell Biol.* 96:1-27.
33. Toyoshima, K., and B. Tandler. 1987. Modified smooth endoplasmic reticulum in type-II cells of rabbit taste buds. *J. Submicrosc. Cytol.* 19:85-92.
34. van Deurs, B., T. I. Tønnessen, O. W. Petersen, K. Sandvig, and S. Olsnes. 1986. Routing of internalized ricin and ricin conjugates to the Golgi complex. *J. Cell Biol.* 102:31-47.
35. Woods, J. W., M. Doriaux, and M. G. Farquhar. 1986. Transferrin receptors recycle to cis and middle as well as trans Golgi cisternae in Ig-secreting myeloma cells. *J. Cell Biol.* 103:277-286.